



# International Journal of Advance Engineering and Research Development

National Conference On Nanomaterials, (NCN-2017)

Volume 4, Special Issue 6, Dec.-2017 (UGC Approved)

## INFLUENCE OF TRANSITION METAL NICKEL ON SEMICONDUCTOR TIN OXIDE

\*T.V.Banumathi<sup>1</sup>, G.Asha<sup>2</sup>

<sup>1</sup>Associate Professor, Department of Physics, Sri G.V.G.Visalakshi College for Women, Udumalpet, Tamil Nadu,

<sup>2</sup>Department of Physics, Sri G.V.G.Visalakshi College for Women, Udumalpet, Tamil Nadu

**Abstract:-** Ni-doped SnO<sub>2</sub> nanoparticles has been synthesized by the co-precipitation method from SnCl<sub>2</sub>·2H<sub>2</sub>O and NiCl<sub>2</sub>·6H<sub>2</sub>O in the present study. Precipitation method is one of the most widely used techniques to produce SnO<sub>2</sub> powders. Structural, morphological and optical properties of the synthesized nanoparticles were studied using X-ray diffraction (XRD), Scanning Electron Microscopy (SEM), UV-VIS Spectroscopy respectively. The X-ray diffraction revealed that the sample is a pure rutile-tetragonal structure and the presence of Nickel has not significantly distorted the Tin oxide. Average crystallite size was calculated from the XRD peak using Debye Scherrer's formula as 12.6 nm and 10.48 nm for x=0.5 and x=0.05 weight percent of Nickel in Sn<sub>1-x</sub>Ni<sub>x</sub>O<sub>2</sub>. The particle size has been identified by Scanning Electron Microscope. The optical band gap for Nickel doped SnO<sub>2</sub> using UV-VIS Spectroscopy has been calculated as 3.74 eV.

**Keywords:** Co-Precipitation, Rutile-tetragonal, SEM, UV-VIS Spectroscopy, Tin -Oxide, Nickel, Crystallite size.

### INTRODUCTION

The physical properties and behaviour of semiconducting transparent metal oxides such as SnO<sub>2</sub>, TiO<sub>2</sub> and ZnO in the recent years at the nanoscale has significantly increased their potential applications. These metal oxides, have attracted a lot of attention due to their outstanding properties especially when they are impregnated with elements having magnetic property. The magnetic, optical, catalytic and electronic properties of materials depend strongly on size, structure and shape of nanoparticles. Another reason for the attraction of scientists' attention towards Nano sized particles is that, they behave differently from bulk materials. With decreasing particle size the band structure of the semiconductors changes. The applications extend as transparent conducting electrode for solar cells, a gas sensing material for gas sensors devices, photochemical and photoconductive devices in liquid crystal display, gas discharge display, lithium-ion batteries. Tin oxide (SnO<sub>2</sub>), normally known as cassiterite, is a typical wide band gap n-type semiconductor (E<sub>g</sub> = 3.6 eV at 25°C) and one of the most widely used semiconductor oxides due to its chemical and mechanical stability<sup>[1,2]</sup>. It has Rutile tetragonal structure. Its high optical transparency, electrical conductivity and chemical sensitivity makes it a very attractive material for solar cells, heat mirrors, catalysis, and gas-sensing applications. Adding new elements and improvising novel functional behaviours to the existing semiconductors by engineering and tailoring their structure, composition and particle/grain size the physical properties are altered which results in the new approaches for enhancing the current applications of semiconductor materials<sup>[3,4]</sup>. Preparation of these materials in the nanoscale size range is more interesting and challenging due to the increased surface-to-volume ratio that might affect the structural and most other physical properties. Transition-metal Nickel has been added to introduce magnetic functionality in the semiconductors. Nanoparticles of tin oxide have been synthesized through different chemical routes, such as precipitation<sup>[5,6]</sup>, sol-gel, hydrolytic<sup>[7,8]</sup> and polymeric precursor methods<sup>[9]</sup>. In this work, the Ni-doped SnO<sub>2</sub> nanoparticles has been synthesized by chemical co-precipitation method with various weight percentage because this method has some advantages such as precise control over the stoichiometry, high purity and high chemical homogeneity.

### 2. EXPERIMENTAL PROCEDURE

Ni doped SnO<sub>2</sub> nanoparticles has been synthesized by chemical co-precipitation method. 96% mole of SnCl<sub>2</sub>·2H<sub>2</sub>O (98% purity, Merck) and 4% of NiCl<sub>2</sub>·2H<sub>2</sub>O (98% purity Merck) has been used as precursor. The materials were dissolved in 100ml of de-ionized water separately and the solutions were mixed in equal proportion. Then ammonia (≥ 25% Merck) was added drop wise into the mixture solution with constant stirring at 30°C until the pH 5 was reached. The precipitate was allowed to settle down for 1 hour. Then it was washed several times by de-ionized water. The precipitate was filtered using filter paper and was subjected to hot air oven at 100°C for 2 hours. The powder was then ground well using a mortar and pestle for 1 hour. The collected sample was annealed in muffle furnace at 400°C for 3 hours. After annealing, the powder was once again pounded using pestle and mortar for 1 hour. The grey coloured powder was extracted as the resultant material. The process was repeated by the same method by varying the concentrations of Nickel.

### 3. RESULTS AND DISCUSSION

#### 3.1 XRD Analysis

The XRD pattern of  $\text{Sn}_{1-x}\text{Ni}_x\text{O}_2$  ( $x = 0.5$  and  $x = 0.05$ ) nanoparticles were recorded in the region of  $2\theta$  between  $0^\circ$  and  $80^\circ$  indicated in the Fig 3.1(a) and Fig 3.1(b). The XRD pattern of Tin oxide exhibits some predominant peaks for the planes (110), (101) and (201) corresponding to  $2\theta = 26.74440^\circ$ ,  $36^\circ$  and  $52^\circ$  respectively. Both diffractograms are characteristic to rutile  $\text{SnO}_2$ . For both Nickel concentration, all peaks are clearly indexed to tetragonal  $\text{SnO}_2$  as per JCPDS file 77-0447<sup>[10]</sup>. No secondary phases are observed, indicating a good Ni integration in the  $\text{SnO}_2$  lattice however it is observed that the increased percentage of Ni has slightly broadened the smaller peaks. The strong and sharp reflection peaks indicate the high crystallinity of Tin Oxide. The average crystallite grain size calculated using Scherrer formula for both the samples are 12.6 nm and 10.48 nm respectively Table I. The lattice parameters 'a' and 'c' calculated for both the samples from the peak positions are  $a = 4.736$ ,  $c = 3.192$  and  $a = 4.714$ ,  $c = 3.170$  respectively Table II. It is found from this calculation that higher is the concentration of 'Ni' in the sample, the increase is in the value of the lattice constants. This leads to an understanding that the Tin Oxide atoms in the lattice have been subjected to squeezing stress which has not distorted the rutile tetragonal structure on the whole.

#### 3.2 Scanning Electron Microscope :

The surface morphology of the nanoparticles was studied by SEM. The scanning electron microscopy (SEM) provided further insight into the morphology and size details of the Nickel doped Tin oxide nanoparticles. Fig.3.2(a) & Fig.3.2 (b) shows the SEM image of the as-synthesized Nickel doped Tin oxide nanoparticles. SEM image of the studied nanoparticles confirms the existence of very small, homogeneously distributed and extremely crystalline nanoparticles. Some particles are of spherical shape with the actual particle size as 120.74 nm, 152.02 nm, 180.56 nm<sup>[11]</sup> as observed under various magnification. The clustering of the particles is observed in Fig.3.2 (c) & Fig.3.2 (d) which is attributed to the Ni atoms squeezing the lattice sites due to higher concentrations.

#### 3.3 UV-VIS Spectroscopy

The Optical absorption measurement was carried out on  $\text{Sn}_{1-x}\text{Ni}_x\text{O}_2$  ( $x = 0.05$ ). Figure 3.3(a) shows the optical UV-VIS absorption spectrum of  $\text{Sn}_{1-x}\text{Ni}_x\text{O}_2$  nanoparticles. The optical absorption coefficient has been measured in the wavelength range of 300-800 nm. From the spectrum the absorbance edge was observed at 352 nm. The higher absorption in the visible region was due to the incorporation of 'Ni' ions in the Tin oxide lattice. The optical band gap energy ( $E_g$ ) of the semiconductor was calculated from Tauc relation. A plot of  $(\alpha h\nu)^2$  versus  $h\nu$  axis shows intermediate linear region; the extrapolation of the linear part can be used to calculate the  $E_g$  from intersect with  $h\nu$  axis as shown in fig 3.3(b). The resultant value of  $E_g$  for  $\text{SnO}_2$  was found to be 3.74 eV.

### 4. ACKNOWLEDGEMENT

The authors acknowledge with thanks the SAIF, CUSAT, Cochin, for providing results of the samples at the earliest submitted for analysis and characterization.

### 5. CONCLUSION

Ni added  $\text{SnO}_2$  Nanopowders  $\text{Sn}_{1-x}\text{Ni}_x\text{O}_2$  has been prepared by Co-precipitation method from  $\text{SnCl}_2 \cdot 2\text{H}_2\text{O}$  and  $\text{NiCl}_2 \cdot 6\text{H}_2\text{O}$ . XRD confirms the formation of nanostructured  $\text{SnO}_2$  with rutile tetragonal structure. XRD measurements indicate the grain size as ranging from 10.48 to 12.6 nm. SEM results show that the particles are agglomerated and they are essentially a cluster of nano particles with the particle size in the range as 120.74 to 180.56 nm. In the UV absorption spectrum of  $\text{SnO}_2$  nanoparticles, the absorbance edge was observed at 352 nm. The optical band gap energy ( $E_g$ ) of the semiconductor calculated from Tauc plot was  $E_g = 3.74\text{ eV}$  which shows an absorption in the near and mid region.

### REFERENCES

- [1] L.I. Nadaf, K.S. Venkatesh, IOSR Journal of Applied Chemistry (IOSR-JAC) e-ISSN: 2278-5736. Volume 9, Issue 2 Ver. I (Feb. 2016), PP 01-04
- [2] Mousa Aliahmad and Mohsen Dehbashi, Iranica Journal of Energy & Environment 4(1) Special Issue on Nanotechnology: 49-52, 2013, ISSN 2079-2115, IJEE an Official Peer Reviewed Journal of Babol Noshirvani University of Technology, DOI:10.5829/idosi.ijee.2013.04.01.08
- [3] Asama. N. Naje, Azhar S. Norry, Abdulla. M. Suhail, ISSN: 2319-8753, Vol. 2, Issue 12, December 2013
- [4] Fang LM, Zu XT, Li ZJ, Zhuc S, Liu CM, Zhou WL, Wang LM, J. Alloys and Compound 454:261 (2008)
- [5] Zhang J, Gao L (2004) J Solid State Chem. 177:1425
- [6] T. Dietl, H. Ohno, F. Matsukura, J. Cibert, and D. Ferrand, Science 287, 1019

- (2000); T. Dietl, H. Ohno, F.Matsukura, Phys. Rev. B 63, 195205 (2001).  
 [7] H. Katayama-Yoshida and K. Sato, J. Phys. Chem.Solids64, 1447 (2003);  
 Semicond. Sci. Technol. 17, 367, (2002).  
 [8] A.C. Bose, D. Kalpana, P. Thangadurai, S. Ramasamy, J. Power Sources 107  
 (2002) 138.  
 [9] N. Segent, P. Gelin, L. Perrier, H. Praliaud, G.Thomas, Sens. Actuators B 84  
 (2002) 176.  
 [10] L. Brousseau, C.V. Santilli, S.H. Pulcinelli, A.F. Craievich, J. Phys. Chem. B 106  
 (2002) 2885.  
 [11] J. Zhang, L. Gao, J. Solid State Chem. 177 (2004) 1425.  
 [12] Z. X. Deng, C. Wang, Y.D. Li, J. Am. Ceram. Soc. 85 (2002) 2837.  
 [13] S. Gnanam et al, digest journal of Nanoparticles and Biostructures.Vol .5 No3  
 (699-704)July-sep(2010).  
 [14] M.M Bagheri et al, Physics. b Vol 403(2431-2437)2008.

### **INFLUENCE OF TRANSITION METAL NICKEL ON SEMICONDUCTOR TIN OXIDE**

**\*T.V. Banumathi<sup>1</sup>, G.Asha<sup>2</sup>**

#### **3.1 XRD Analysis**

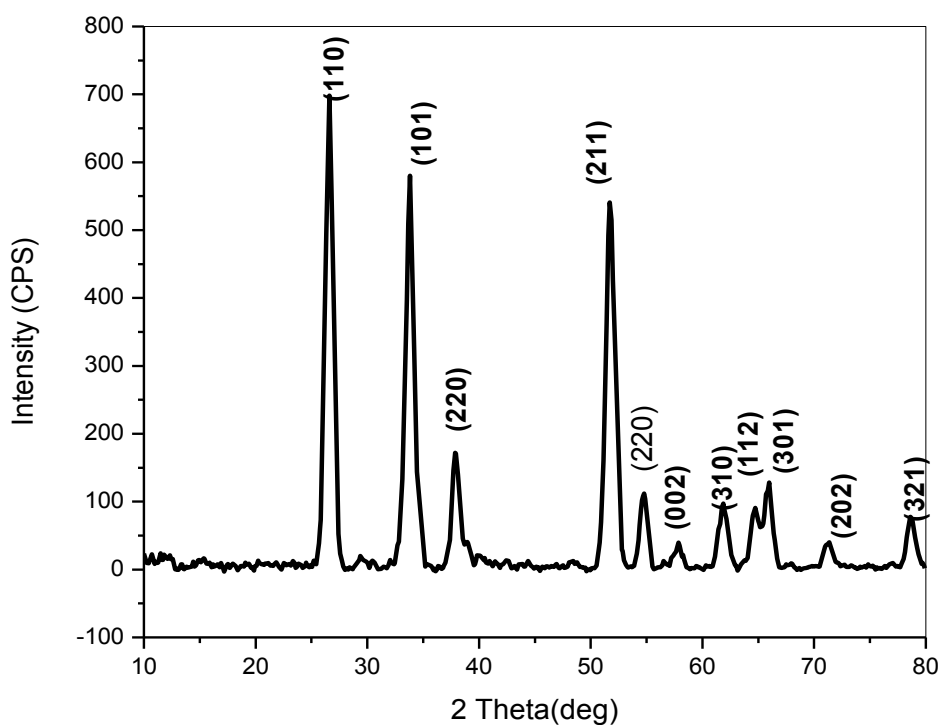


**Fig 3.1(a) XRD pattern of  $\text{Sn}_{1-x}\text{Ni}_x\text{O}_2$  ( $x = 0.5$ )**

# INFLUENCE OF TRANSITION METAL NICKEL ON SEMICONDUCTOR TIN OXIDE

\*T.V. Banumathi<sup>1</sup>, G.Asha<sup>2</sup>

## 3.1 XRD Analysis

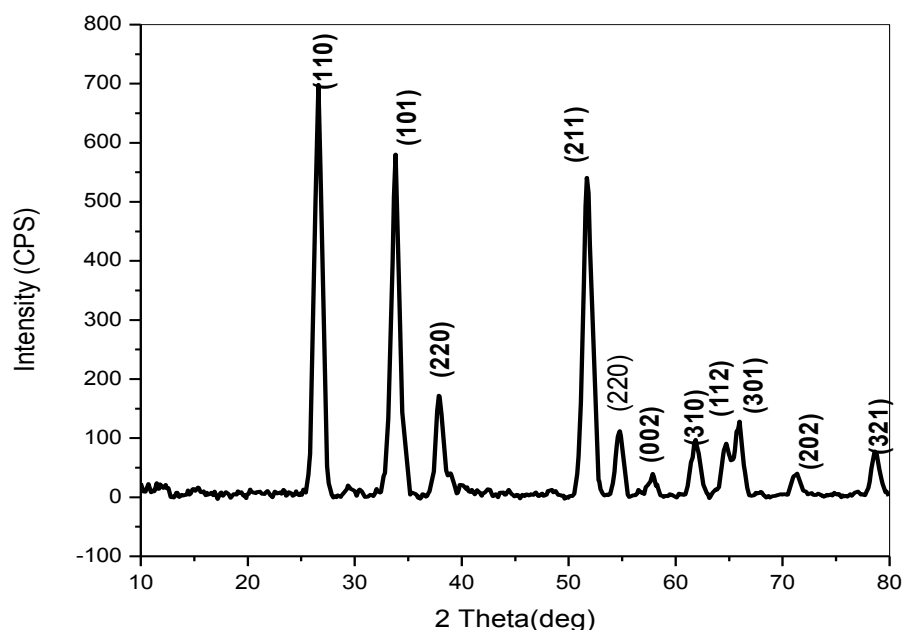


Fig 3.1(b) XRD pattern of  $\text{Sn}_{1-x}\text{Ni}_x\text{O}_2$  ( $x = 0.05$ )

# INFLUENCE OF TRANSITION METAL NICKEL ON SEMICONDUCTOR TIN OXIDE

\*T.V. Banumathi<sup>1</sup>, G.Asha<sup>2</sup>

Table I Grain size of  $\text{Sn}_{1-x}\text{Ni}_x\text{O}_2$  ( $x = 0.5$  &  $x = 0.05$ )

# INFLUENCE OF TRANSITION METAL NICKEL ON SEMICONDUCTOR TIN OXIDE

T.V. Banumathi<sup>1</sup>, G.Asha<sup>2</sup>

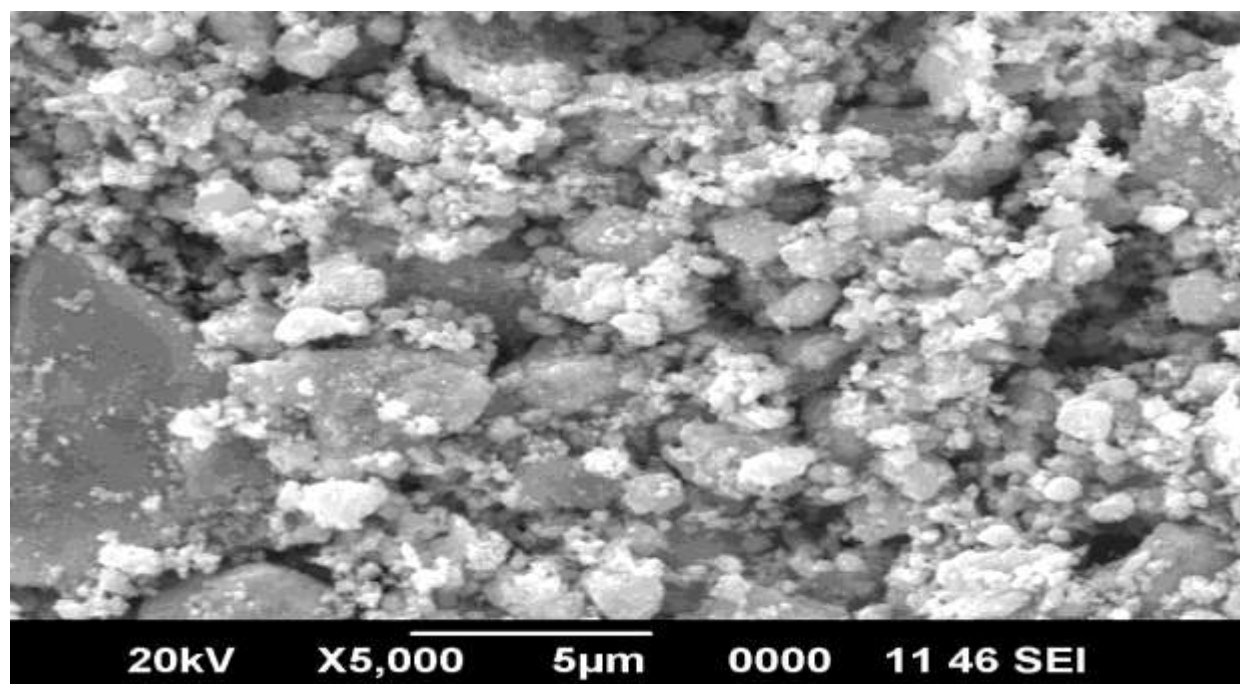
Sample	h k l	FWHM (deg)	d-spacing ( $\text{\AA}$ )	Grain size (nm)	Lattice Constant		Standard Values ( $\text{\AA}$ )
					a ( $\text{\AA}$ )	c ( $\text{\AA}$ )	
$\text{Sn}_{1-x}\text{Ni}_x\text{O}_2$ ( $x=0.5$ )	110	0.674	3.34910	12.24	4.736	3.192	a = 4.738 c = 3.188
	101	0.800	2.64670	10.13	4.738	3.190	
	211	0.795	1.76546	9.63	4.740	3.191	
	101	0.800	2.64670	0.13	4.740	3.191	
	200	0.666	2.3730	12.04	4.740	3.191	
$\text{Sn}_{1-x}\text{Ni}_x\text{O}_2$ ( $x=0.05$ )	110	0.5258	3.33065	15.5	4.714	3.170	a = 4.738 c = 3.188
	101	0.5279	2.63133	15.3	4.714	3.170	
	211	0.54050	1.75583	14.1	4.727	3.170	
	101	0.52790	2.63133	15.3	4.727	3.170	
	211	0.54050	1.75583	14.1	4.727	3.180	
	202	0.56270	1.31882	6.89	4.727	3.180	

Table II Lattice parameters of  $\text{Sn}_{1-x}\text{Ni}_x\text{O}_2$  ( $x = 0.05$  and  $x = 0.5$ )

# **INFLUENCE OF TRANSITION METAL NICKEL ON SEMICONDUCTOR TIN OXIDE**

T.V. Banumathi<sup>1</sup>, G.Asha<sup>2</sup>

3.2 Scanning Electron Microscopy



**Fig. 3.2 (a) SEM Micrograph of  $\text{Sn}_{1-x}\text{Ni}_x\text{O}_2$  ( $x=0.05$ )**

# **INFLUENCE OF TRANSITION METAL NICKEL ON SEMICONDUCTOR TIN OXIDE**

T.V. Banumathi<sup>1</sup>, G.Asha<sup>2</sup>

3.2 Scanning Electron Microscopy

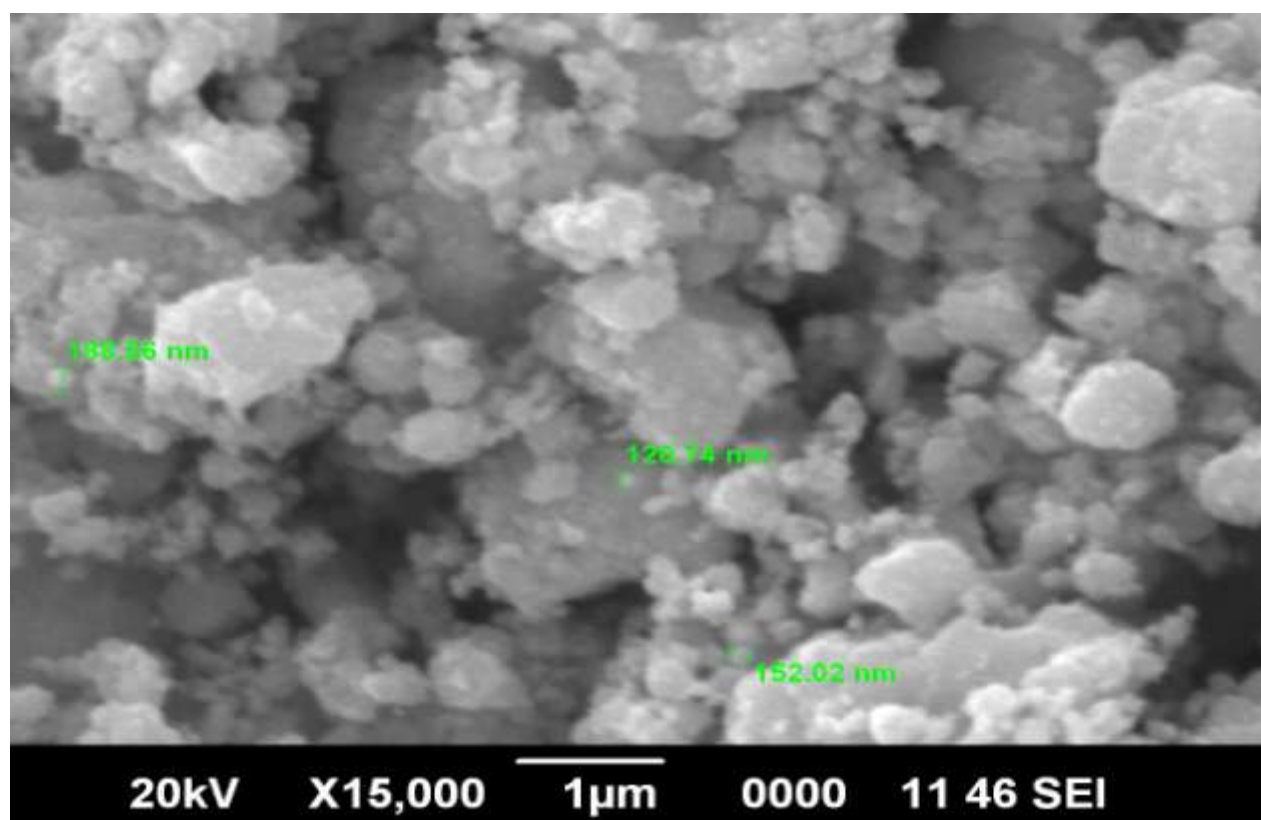


**Fig. 3.2 (b) SEM Micrograph of  $\text{Sn}_{1-x}\text{Ni}_x\text{O}_2$  ( $x=0.05$ )**



**INFLUENCE OF TRANSITION METAL NICKEL ON  
SEMICONDUCTOR TIN OXIDE**

**T.V. Banumathi<sup>1</sup>, G.Asha<sup>2</sup>**

**3.2 Scanning Electron Microscopy**

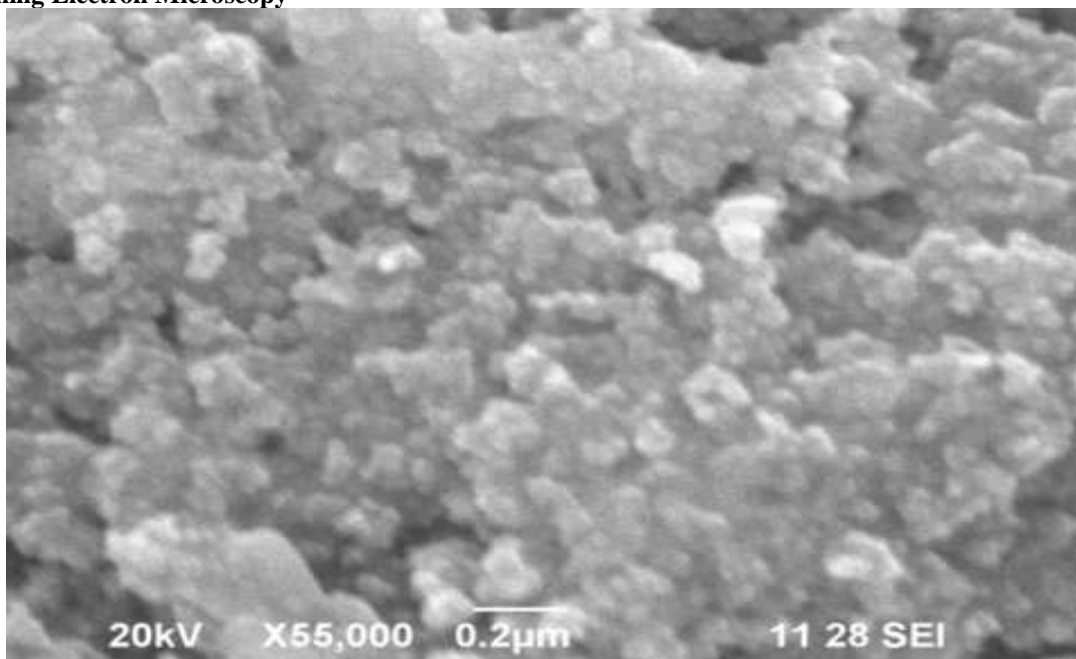


**Fig. 3.2 (c) SEM Micrograph of  $\text{Sn}_{1-x}\text{Ni}_x\text{O}_2$  (x=0.5)**

**INFLUENCE OF TRANSITION METAL NICKEL ON  
SEMICONDUCTOR TIN OXIDE**

**T.V. Banumathi<sup>1</sup>, G.Asha<sup>2</sup>**

**3.2 Scanning Electron Microscopy**

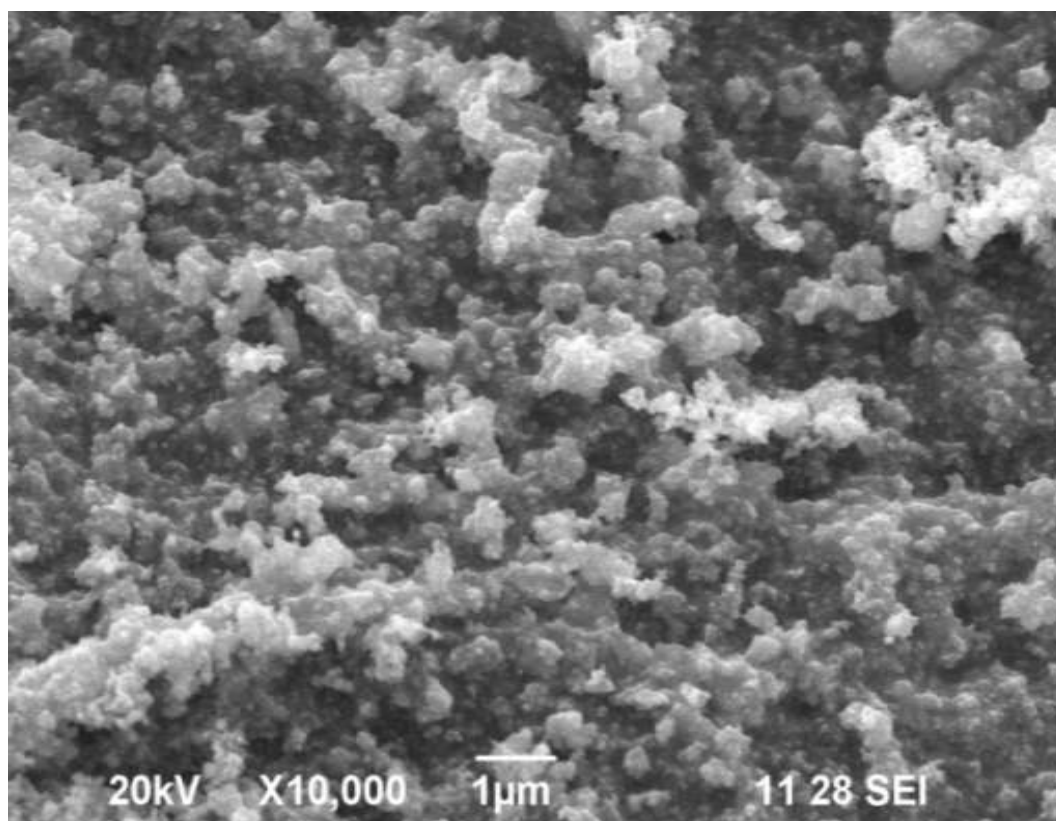


**Fig. 3.2 (d) SEM Micrograph of  $\text{Sn}_{1-x}\text{Ni}_x\text{O}_2$  (x=0.5)**

# INFLUENCE OF TRANSITION METAL NICKEL ON SEMICONDUCTOR TIN OXIDE

T.V. Banumathi<sup>1</sup>, G.Asha<sup>2</sup>

## 3.3 UV-VIS Spectroscopy

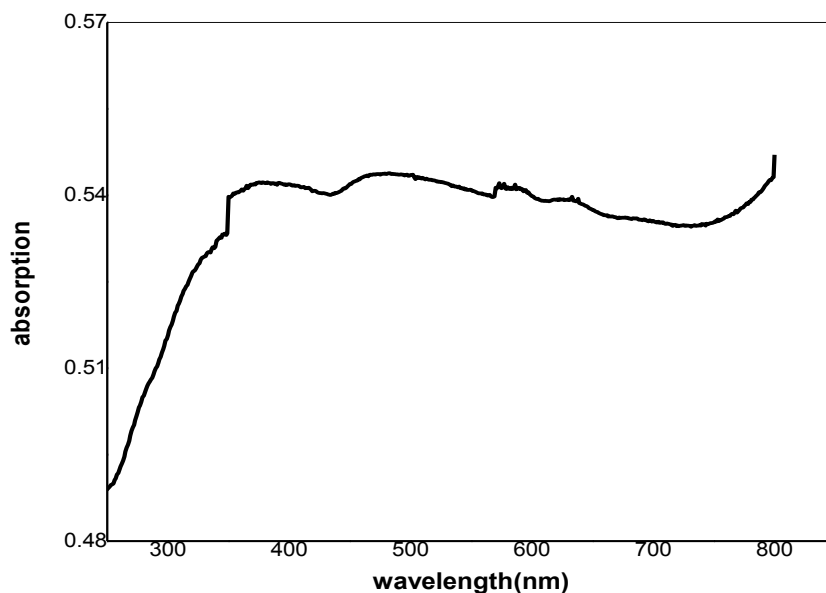


Fig. 3.3(a) The absorption spectrum of SnO<sub>2</sub>

# INFLUENCE OF TRANSITION METAL NICKEL ON SEMICONDUCTOR TIN OXIDE

T.V. Banumathi<sup>1</sup>, G.Asha<sup>2</sup>

## 3.3 UV-VIS Spectroscopy

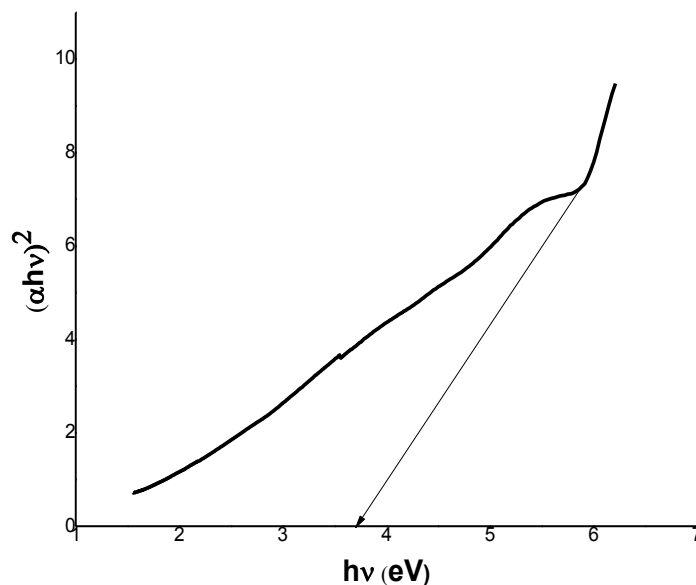


Fig.3.3(b) Plot of  $(\alpha h\nu)^2$  verses photon energy  $h\nu$